Preprint of the paper published in Int.J.Appl.Ceram.Technol 2020, 17:1752-1760

Preparation of GdBCO precursor powder by spray-drying a nitrate solution containing PEG

J.Camps[1], J.Farjas[1], P.Roura-Grabulosa[1*], A.Calleja[2]

[1]University of Girona, Campus Montilivi, Edif.PII, E-17174 Girona, Catalonia, Spain

[2]Oxolutia S.L. Avda.Castell de Barberà 26, Barberà del Vallès, 08210, Barcelona, Spain

* Corresponding author: pere.roura@udg.cat

Several precursor powders, obtained after precipitation from metal nitrate solution containing polyethylene glycol (PEG) (inside a Pyrex glass reactor or by spray-drying), and their thermal evolution to GdBCO were analyzed by thermogravimetry (TG), differential thermal analysis (DTA), Fourier transform infrared spectroscopy (FTIR) and X-ray diffraction (XRD). The amount of PEG had a crucial role in the $BaCO_3$ content of the "Kjeldahl precursors" but a minor effect on the degree of transformation to GdBCO at 900ºC, which did not reach completion after 1 h. In contrast, a low-PEG spray-dried powder led to almost 100% GdBCO in only 5 min. The high degree of cation dispersion reached by spray-drying and the coexistence with a liquid phase can explain this short reaction time. The spray-dried powder compares favorably with the mechanical mix of metal oxides and Ba carbonate that is commonly used as precursor powder for the synthesis following a solid-state reaction.

1. Introduction

$YBa_2Cu_3O_{6+x}$ (YBCO) has attracted much attention since the discovery of high-temperature superconductivity in 1986 and, among other REBCO compounds (RE = rare-earth) it is the first candidate for large scale applications [1] such as coated conductors, magnetic shields, superconducting motors, etc. Substitution of Y by Gd leads to a significant improvement of the superconducting properties [2]: higher transition temperature, larger critical current density at high magnetic fields and higher ability for trapping the magnetic field.

These compounds can be synthesized as powders that find application as "raw materials" for the fabrication of bulk compacts by sintering them in the solid state [3], for melt processing of highly textured ingots [4,5,6], as raw material to obtain fluorinated precursors for the synthesis of thin films through the trifluoroacetate (TFA) route [7], and to build targets for pulsed laser deposition (PLD) of REBCO thin films [8].

The most direct way to obtain powders is by reaction of the elementary oxides (CuO, RE_2O_3) and $BaCO_3$ in the solid state. This procedure requires grinding, calcining and sintering steps lasting tens of hours to ensure complete decomposition of $BaCO_3$ and reaction leading to the superconductor phase without any secondary phase.

To reduce the processing time, alternative methods have been developed that aim at reaching high dispersion of the different cations thus improving their reactivity. These methods begin with a solution containing the cations, and face the problem of the reduced solubility of Ba compounds and the difficulty to avoid segregation during precipitation.

Cation dispersion can be achieved by the sol-gel route (Pechini method [9]) by adding complexing or jellifying agents that upon reaction incorporate the cations in a gel. The high organic content leads to CO_2 release during gel pyrolysis and formation of a large fraction of $BaCO_3$ that needs to be decomposed at high temperature [10,11]. Another possibility is the addition of a polymer in the solution (polymer assisted deposition or PAD [12]). After solvent evaporation, the cations are trapped in the highly-viscous polymer. Among other polymers, polyvinyl alcohol (PVA) has been used for this purpose [4,13]. Despite the dispersant role of PVA, partial segregation of Ba could not be avoided [4].

The present paper reports on the use of polyethylene glycol (PEG) in a solution of Ba, Cu and Gd nitrates with the aim of preparing GdBCO powder. The role of PEG is twofold. On the one hand, it acts as a complexing agent, thus increasing Ba solubility [14]. On the other hand, it acts as surfactant reducing the solution's viscosity what allows the formation of a finer liquid aerosol during atomization by spray drying. After drying, the precursor powder is expected to contain a more intimate mix of cations. In addition, the oxygen atoms in the PEG

backbone chain reduce the chances to get a carbonaceous residue during pyrolysis and reduce the decomposition temperature [15]. The structure and thermal evolution of the precursor powder obtained by spray-drying are compared with those obtained by precipitation in a Pyrex glass reactor and with the mix of metal oxide and Ba carbonate powders.

2. Experimental section

2.a Powder precursors preparation

The preparation of all precursor powders begun with CuO (Diopma, 99.9%), $BaCO_3$ (Alfa Aesar 99%) and Gd_2O_3 (99.9%) commercial powders. Polyethylene glycol (PEG) of molecular mass 8000 amu (Sigma Aldrich) was added at different concentrations to enhance their solubility in a solution of nitric acid (65% Merck).

Ceramic Powder A was obtained mixing stoichiometric amounts of CuO, $BaCO_3$ and Gd_2O_3 and grinding them with a mortar and pestle.

Powder B was prepared by dissolution of these oxides in a 1 M solution of HNO_3 in water with an amount of PEG equivalent to a four $–CH_2CH_2O–$ units of PEG, for 1 mol of metals ("4/1 molar ratio"). The procedure was as follows. First, the Cu and Gd oxides were dissolved in a solution with a slight excess of nitric acid, which was stirred and heated at 80ºC until it became clear and deep blue. Then, in another baker, Ba carbonate was dissolved at room temperature in a similar solution of nitric acid until bubbling diminished. Then, the solution was heated at 80ºC until it became clear. These two solutions were then mixed with a solution of PEG at 80ºC. The resulting clear pale blue solution containing 0.4 M metal cations remained stable at room temperature. It was introduced in a Pyrex glass reactor and heated to 370ºC until complete evaporation of the solvent.

Powder C was similar to Powder B but with a lower PEG content (0.3/1 molar ratio).

Finally, Powder D was obtained from the same solution as that used for Powder C. In this case, the solution was introduced in a spray dryer. It was sprayed at an air pressure of 4 bar with a needle frequency of 0.25 Hz and the aerosol was dried at 240ºC. The powder was collected thanks to a small cyclone of 12 cm in diameter.

The as-prepared A, B and C powders were loose and black whereas Powder D was pale green and somewhat sticky as if it retained water and PEG within its particles.

2.b Heat treatments

The powders were heat-treated in atmospheric air with an electric furnace. An amount of about 100 mg was put inside an alumina crucible and, then, introduced in the furnace which was

previously thermalized at the programmed temperature. After the time required for the heat treatment (5 minutes or 1 hour), the crucible was taken out and put in contact with a metallic block to ensure rapid quenching. At the highest temperature (900ºC) the powder retracted to the center of the crucible, and the cylinder that resulted could be easily extracted from it and ground with a mortar and pestle without much effort. No signs of extensive melting were observed.

2.c Thermal and structural analyses

The mass evolution of the precursor powders when heated at 10 K/min in synthetic air was recorded by thermogravimetry (TG) with the Setsys Evolution apparatus of Setaram. The measured curve was subtracted from one curve measured at the same conditions but with an empty alumina crucible (blank curve). The same apparatus measured the heat exchanged (Differential Thermal Analysis, DTA).

XRD analyses were performed with the powder diffractometer XRD-Advance of Bruker, working with a Cu source in the Bragg-Brentano configuration.

FTIR spectra were acquired with a Mattson Satellite spectrophotometer by Attenuated Total Reflectance technique (diamond ATR crystal) at 4 cm^{-1} resolution.

Finally, SEM micrographs have been obtained with the ZEISS DSM 960A microscope to observe the morphology of the powders, which were deposited on a conductive tape.

3. Results

3.a Ceramic Powder A

The aspect of this powder as seen by SEM is shown in Fig.2a. When the ceramic Powder A was heated inside the TG apparatus, the recorded mass remained constant up to around 750ºC. Above this temperature, a continuous mass-loss process can be observed in the corresponding TG curve (Fig.3a). This process is due to the decarbonation of $BaCO_3$.

After heating the powder at 850ºC for 1 h, the CuO and Gd_2O_3 phases of the as-mixed powder (Fig.1) have completely disappeared and a residual fraction of $BaCO_3$ is still detected (Fig.4). The XRD curve is dominated by the GdBCO phase. At 900ºC, one can observe a further reduction of the $BaCO_3$ main peak, which becomes almost undetectable above the noise level.

3.b Powder B: high PEG to metal ratio (4/1)

XRD of the precursor Powder B reveals a rich phase structure containing Gd_2O_3, CuO, Cu, $BaCO_3$, $Ba(NO_3)_2$ and BaO_2 (Fig.1). At room temperature, all metals are expected to precipitate during solvent evaporation as nitrates. However, at the nominal temperature of the glass reactor (370ºC), decomposition of Gd and Cu nitrates is expected to occur, what is confirmed by detection of their oxides. In contrast, more stable Ba nitrate should remain. Detection of $BaCO_3$ indicates that Ba nitrate has partially decomposed. Since the reactor temperature is not high enough to decompose it, we consider that overheating has occurred due to combustion between nitrates and PEG.

Upon further heating of this precursor powder, successive decomposition of Ba nitrate and Ba carbonate are expected. So, the two mass-loss steps observed in the TG curve (Fig.3) have this origin; the one beginning at about 500ºC corresponds to nitrate decomposition and the other one, beginning at 750ºC, to carbonate decomposition.

If we take the final mass, m_f, of the TG curve (Fig.3) as reference, and consider that the phases at this point are almost 100% oxides at their maximum oxidation state, then we can estimate the fraction of the Ba atoms residing in the carbonate before its decomposition (say at T = 700ºC). From the molar mass of the oxides and Ba carbonate, we can state that:

$$\frac{Ba\ in\ BaCO_3\ at\ T}{Ba\ total} = \frac{m(T)-m_{OX}}{m_{CA}-m_{OX}} = 50\%, \qquad (1)$$

where m_{OX} is the mass of all-oxides (726.6 amu) and m_{CA}, that of $GdO_{1.5}$+2$BaCO_3$+3CuO (814.6 amu).

According to the XRD measurements of this powder (Fig.5), after 1 h at 800ºC the main changes of the precursor powder have been the disappearance of Ba nitrate and the formation of GdBCO by subsequent reaction with CuO and Gd_2O_3. A residual amount of Gd_2BaCuO_5 has been also formed. From the approximate relative amount of the Ba-containing phases determined from the XRD curve ($BaCO_3$ 27%, GdBCO 35%, Gd_2BaCuO_5 2%, BaO_2 4%) we can again estimate the fraction of Ba atoms in carbonate (55%). The result is in fair agreement with the estimation from the TG curve.

When compared with the ceramic Powder A, we observe that at 900ºC a significant amount of secondary phases (Gd_2BaCuO_5 and CuO) still coexists with GdBCO. Since Gd_2BaCuO_5 has less Cu that GdBCO, CuO is also detected.

3.c Powder C: low PEG/metal ratio (0.3/1)

In contrast with Powder B, Ba nitrate has not decomposed. Presumably the PEG content in Powder C was not high enough to trigger combustion inside the glass reactor and, consequently, no overheating is expected above the nominal reaction temperature of 370ºC. Furthermore, the absence of combustion can also explain why Cu atoms have remained in the Cu(II) oxidation state and have not been partially reduced to metallic copper as it occurred in Powder B [16].

No Gd-containing phase has been detected by XRD Powder C (Fig.1). The natural question is where these atoms reside. Since the XRD curve of Powder C is very simple (it only contains Ba nitrate and CuO peaks), we can infer the state of Gd atoms from the TG curve (Fig.3). If all phases at 950ºC are oxides, then we can predict the normalized mass of Gd_2O_3, CuO and $Ba(NO_3)_2$ phases from the normalized mass at the end of the TG curve (0.775). The result (0.99) almost coincides with the normalized mass of the TG curve at 350ºC. In other words, we can conclude that Gd atoms are in the form of Gd_2O_3 and that they are not detected by XRD because of their nanocrystalline nature. Furthermore, the good agreement between prediction and experiment tells us that, at 370ºC, PEG has completely decomposed. Independent TG measurements on PEG alone have shown that its decomposition in air finishes at 280ºC.

The TG curve of Powder C has the same two-step shape than that of Powder B. Given the same interpretation, we can apply here Eq.(1) to estimate the ratio of Ba atoms in carbonate. This quantity (33%) is significantly lower than that of Powder B.

The XRD curve at 800ºC (Fig.6) confirms that $BaCO_3$ is much less abundant in Powder C than in Powder B and this rapport continues at 850ºC. At 900ºC, the curves of both powders are very similar; they reveal the existence of Gd_2BaCuO_5.

Up to this point, we have arrived at the unexpected conclusion that the precursor powders obtained from nitrates with the addition of PEG find difficulties to react to form GdBCO, after precipitation in the glass reactor. A fraction of these powders is transformed to the Gd_2BaCuO_5 non-equilibrium intermediate phase that still survives after annealing at 900ºC for 1 h. In contrast, the ceramic powder leads to complete transformation to GdBCO after the same heat treatment.

Concerning $BaCO_3$, as the temperature is increased, in Powder C this phase decomposes similarly than in the ceramic powder, whereas it is delayed to higher temperature in Powder B. For this reason, we choose the PEG to metal ratio 0.3/1 of Powder C to improve the reactivity of the phases with the spray-drying precipitation method.

3.d Powder D: spray-dried

The aspect of the spray-dried power is shown in Fig.2c. The bright particles of around 1 μm in diameter are presumably the product of individual sprayed droplets. XRD of this powder delivers very short information about its phases (Fig.1), Ba nitrate being the only one unambiguously detected. The nature of the Gd- and Cu-containing phases is unknown except that they are presumably amorphous. Fortunately, relevant information can be obtained by FTIR and thermogravimetry.

The IR spectrum of Fig.7 delivers crucial information to identify the state of copper as Cu hydroxynitrate [$Cu_2(OH)_3NO_3$]. The most significant vibrational mode is that giving a narrow peak at 3544 cm^{-1} that is associated with OH- groups inside the layers of this compound [17]. This peak appears superimposed onto a broad band of unbound OH- groups that are located in the inter-lamellar space. The identification of this copper salt is further confirmed by detection of the N-O stretching mode of a monodentate O-NO_2 group at 1045 cm^{-1} [17]. Finally, the color of the precursor (pale-green) coincides with the description given in ref.[17]. In addition to the vibrations of the copper salt, several bands reveal that PEG has not decomposed (C-H and C-O stretching modes at 2920 cm^{-1} and 1080 cm^{-1}, respectively).

The TG curve measured on this powder has been plotted in Fig.3b, together with the DTA curve. In addition to the steps of Ba nitrate and Ba carbonate decomposition already found in powders B and C, a progressive mass-loss process beginning around 100ºC (corresponding to bonded water molecules) and an abrupt process at 270ºC are also detected. The DTA curve reveals that this last process is highly exothermic (e.g. ref.[18] and the DTA signal of Ba nitrate decomposition in Fig.3b). In fact, it is the only exothermic process detected on this powder. Since nitrate decomposition is endothermic, this process must involve reaction with PEG, the sharp DTA peak and abrupt mass-loss step indicating that combustion between nitrates and PEG has occurred. We can thus conclude that above 270ºC no PEG remains.

The horizontal dotted lines drawn in Fig.3 are the sample mass for several chemical compositions, calculated with the assumption that all phases are oxides at 950ºC. The mass predicted for all-nitrates is higher than the experimental value after water-loss. However, if we consider that Cu is in the hydroxynitrate form deduced from FTIR, the predicted mass agrees with the experiment. We thus conclude that precursor powder D (spray-dried at a temperature lower than the combustion process shown in the TG curve), contains PEG, Ba nitrate, Gd nitrate and Cu hydroxynitrate.

After combustion, in the hypothesis that Ba nitrate is the only phase containing Ba the expected mass is higher than that measured, meaning that the local high temperature due to

combustion has partially decomposed it to carbonate. This transformation is similar to what occurred inside the glass reactor during precipitation of Powder B.

Finally, the discrepancy between the expected mass for Ba carbonate plus Cu and Gd oxides and the experimental mass at 700-800ºC means that, after Ba nitrate decomposition, a significant fraction of the sample has already reacted to form GdBCO, as already observed in B and C powders.

After the heat treatment at 900ºC for 1 h, the spray-dried powder does not contain any significant secondary phase (Fig.8) what represents a clear improvement with respect to the other nitrate precursor powders. However, the most relevant result, that indicates the high reactivity of Powder D, is that 5 min at 900ºC is enough to obtain nearly 100% GdBCO (Fig.8). With the same short heat treatment, reaction of ceramic Powder A is far from completion (Fig.4). The aspect of the two products is also very different as revealed by SEM (Figs.2b and 2d). In particular, remark that treated Powder D still remembers its origin from small droplets (Fig.2d). In the inset, the hollow shape of the particles, typical of this drying process, is highlighted.

Before leaving this section, let us have a last look at the TG/DTA plot of Powder D (Fig.3b). The high-temperature portion of the DTA curve has been expanded to show the low-enthalpic endothermic peaks involved in the formation of GdBCO. When the sample of this TG experiment has been heated again, to check the completion of the reaction, these peaks have disappeared. This means that the reaction has reached completion during the first heating ramp (and subsequent cooling) that, at 20 K/min, lasts 5 min above 900ºC.

4. Discussion

4a. Formation of $BaCO_3$

With precipitation from an aqueous solution of metal nitrates with PEG, we expected to get two advantages with respect to the ceramic Powder A: first, avoiding the $BaCO_3$ phase thanks to nitrate precipitation and, second, obtaining a better mixing of cations thanks to precipitation inside a viscous polymer.

With the precursor Powder B we chose a ratio of positive charges (of metal cations) to polymer units (13/4) close to the optimum value (4/1) for polymer assisted deposition process found by Gülgun et al. [13]. However, PEG or its products of decomposition reacted with $Ba(NO_3)_2$ giving $BaCO_3$, and this reaction presumably occurred during a combustion process inside the glass reactor resulting in a high content of Ba carbonate. According to the diffraction

curve of the precursor Powder B (Fig.1) Ba carbonate is more abundant than Ba nitrate. One arrives to the same conclusion when the TG curve (Fig.3a) is analyzed.

The drastic reduction of PEG content during preparation of the precursor Powder C precludes combustion, and allows the thermal decomposition of PEG to occur before Ba nitrate decomposition. The result is a carbonate-free precursor powder. Thus, the question is what is the origin of the carbon atoms leading to carbonate formation during Ba nitrate decomposition when Powder C is heat-treated? The simpler explanation is the carbonaceous residue left behind by PEG.

We performed an additional experiment to reveal the amount of residual carbon formed due to PEG decomposition. We heated two binary powders with the same composition as powders B and C but without copper. Since, in contrast with the dark color or CuO, the powders of Gd_2O_3, $Ba(NO_3)_2$ and $BaCO_3$ are white, the brighter aspect of the "binary Powder C" at 370ºC and 600ºC (Fig.9) tells us that it contains much less carbonaceous residue.

In both powders B and C the amount of $BaCO_3$ is lower than in the ceramic Powder A. So, it is surprising that Powder A transforms quicker to GdBCO (i.e. its transformation reaches completion at 900ºC for 1 h – Fig.1). In fact, the main problem of powders B and C is not the amount of Ba carbonate but their reaction path leading to non-equilibrium phases like Gd_2BaCuO_5 (Figs.5 and 6). When the composition of GdBCO is compared to that of Gd_2BaCuO_5, one is led to think that, during precipitation, some cation segregation has occurred as already observed by other authors with PVA [4], with Gd-rich zones, where nucleation of Gd_2BaCuO_5 has been favored. So, the easiest formation of GdBCO from the spray-dried precursor D, when compared with powder C, seems to be related with a better cation dispersion.

4b. Formation of GdBCO

The formation mechanism of YBCO through intermediate liquid phases has been suggested to occur since long time ago by several authors [19,20,21]. The rationale was to propose that, after decomposition of Ba carbonate, $BaCuO_2$ is formed and that, once above the eutectic temperature, T_E, the $BaCuO_2$-CuO liquid phase reacts with Y_2O_3. This growth mechanism has been kept, however, controversial since strong discrepancies have been detected concerning the temperatures where YBCO is formed. Although Chu et al. [19] published a phase diagram for films shifted to lower temperatures with respect to the bulk phase diagram [22], our own measurements on powders and films indicate a possible temperature downshift by only several tens of Celsius [23].

Since the mechanism involving a liquid phase seems to be acceptable when thermal annealing is made above T_E (around 890ºC in air [24]), it can be in principle directly translated to GdBCO powder formation. During our experiments, we can know when melting occurs thanks to the DTA signal. For both Powder A and Powder D three endothermic peaks are detected above 800ºC (Fig.3). The peak labelled "a" is due to the orthorhombic to hexagonal phase change of Ba carbonate [25, 26], whereas peaks "b" and "c" correspond to the eutectic melting and to the liquidus line of the $BaCuO_2$-CuO phase diagram. When the sample of Powder D used in the TG/DTA experiment of Fig.3b was heated again, all these peaks disappeared indicating that full reaction to GdBCO was reached during the 5 minutes the sample had been partially melted at the first heating ramp. In contrast, in Powder A, peak "a" was still detected (although much less intense) at the second heating ramp. These DTA results agree with the XRD measurements carried out at 900ºC for 5 min (Figs.4 and 8) and indicate that fast reaction occurs in Powder D thanks to the liquid.

Below the eutectic temperature (e.g. at 800ºC), GdBCO was already formed in all powders. Since the XRD curves at 800ºC in Figs.4-5-6-7 already discussed above were measured after an isothermal period of 1 h, no information can be extracted about the reaction rate. For this purpose, we did an additional experiment on Powder C. It was heated at 10 K/min up to 700ºC, where Ba nitrate was completely decomposed (Fig.3a), and it was cooled down quickly. The corresponding XRD curve (Fig.6) reveals an important amount of GdBCO (approx. 35%). If one takes into account that the temperature of this experiment was much lower than for the reaction above T_E, one can conclude that formation of GdBCO is very fast between 630 ºC (the end of Ba nitrate decomposition) and 700ºC or that it has been formed during Ba nitrate decomposition. Formation of YBCO films from fluorine-free metalorganic solutions at temperatures below 700ºC has also been reported at oxygen partial pressures below that of air. In that case, it coincided with the process of Ba carbonate decomposition [21]. So, we are tempted to draw the conclusion that GdBCO (or YBCO) is formed as soon as Ba carbonate or Ba nitrate begin to decompose, allowing its synthesis at very low temperature.

5. Summary and conclusion

PEG has been used to prepare precursor powders for GdBCO synthesis by spray-drying aqueous solutions of the metal nitrates. Preliminary studies involving precipitation inside a glass reactor have served to analyze the role of PEG on precursor formation and its evolution with temperature. A high PEG to metal ratio of 4/1 led to combustion during precipitation and, consequently, a high content of Ba carbonate appeared in the precursor powder. With less PEG

(0.3/1), combustion did not occur and a suitable carbonate-free precursor was obtained. However, the carbonaceous residue, left behind by PEG during precipitation, reacted during Ba nitrate decomposition to form Ba carbonate. Although Ba carbonate was fully decomposed after 1 h at 900ºC, the GdBCO phase was accompanied by the non-equilibrium Gd_2BaCuO_5 phase, probably due to Ba segregation during the precipitation step.

When the solution with less PEG was spray-dried, Gd and Cu atoms remained in an amorphous precipitate of nitrate and hydroxynitrate, respectively. Apparently, the higher degree of cation dispersion, usually related with amorphous phases, was at the origin of the fast reaction leading to almost 100% GdBCO after 5 min at 900ºC. At this temperature, coexistence with the $BaCuO_2$-CuO eutectic liquid also enhanced the reaction rate.

Our study has shown that spray-dried precursor powders are a good alternative to the common mechanical mixture of precursor oxides for the synthesis of GdBCO powder. It also makes clear that eutectic melting enhances GdBCO growth; a result that is relevant in view of the present interest to develop suitable methods for preparing REBCO films from fluorine-free precursors [27].

Acknowledgements

This work has been funded by the Spanish Programa Nacional de Materiales through projects MAT2014-51778-C2-2-R, and RTI2018-095853-B-C22, by the Generalitat de Catalunya contract No. 2017-SGR001519 and by the Universitat de Girona contract No. MPCUdG2016/059.

References:

[1] Freyhardt H C, YBaCuO and REBaCuO HTS for applications. Int.J.Appl.Ceram.Technol. 2007; 4: 203-2016.

[2] Jin L H, Lu Y F, Yan W W, Yu Z M, Wang Y and Li C S, Fabrication of GdBa2Cu3O7-x films by TFA-MOD process. J.Alloys Comp. 2011; 509: 3353-3356.

[3] Awad R, Abou Aly A I, Mohammed N H, Isber S, Motaweh H A and El-Said Bakeer D, Physical and Mechanical Properties of GdBa2Cu3O7-delta Added with Nanosized CoFe2O4 J.Alloys Comp. 2014; 610: 614-622.

[4] Serradilla I G, Calleja A, Capdevila X G, Segarra M, Mendoza E, Teva J, Granados X, Obradors X and Espiell F, Synthesizing the Y-123/Y-211 composite by the PVA method. Supercond.Sci.Technol. 2002; 15: 566-571.

[5] Muralidhar M, Tomita M, Suzuki K, Jirsa M, Fukumoto Y and Ishihara A, A low-cost batch process for high-performance melt-textured GdBaCuO pellets Supercond.Sci.Technol. 2010; 23: 045033.
[6] Pinc J, Bartunek V, Kubasek J, Plechacek V and Hlasek T, Comparison of Mechanical and Superconducting Properties of YBaCuO and GdBaCuO Single Grains Prepared by Top-Seeded Melt Growth. J.Supercond.Nov.Magn. 2016; 29: 1773-1778.
[7] Roma N, Morlens S, Ricart S, Zalamova K, Moreto J M, Pomar A, Puig T and Obradors X, Acid anhydrides: a simple route to highly pure organometallic solutions for superconducting films. Supercond.Sci.Technol. 2006; 19: 521-527.
[8] Rizzo F, Augieri A, Kursumovic A, Bianchetti M, Opherden L, Sieger M, Hühne R, Hänisch J, Meledin A, Van Tendeloo G, MacManus-Driscoll J L and Celentano G. Pushing the limits of applicability of REBCO coated conductor films through fine chemical tuning and nanoengineering of inclusions. Nanoscale 2018; 10: 8187-8195.
[9] Pechini M, US Patent 3330697.
[10] Motta M, Deimling C V, Saeki M J and Lisboa-Filho P N, Chelating agent effects in the synthesis of mesoscopic-size superconducting particles. J.Sol-gel.Sci.Technol. 2008; 46: 201-207.
[11] Kargar M, Alikhanzadeh-Arani S and Salavati-Niasari M, Synthesis of Ultrafine High-T-C Superconducting GdBa2Cu3O7-x Powder. EEE Trans.Appl.Supercond. 2015; 25: 720056.
[12] Burrell A K, McCleskey T M and Jia Q X, Polymer assisted deposition. Chem.Commun. 2008;11: 1271-1277.
[13] Gulgun M A, Nguyen M H and Kriven W M, Polymerized organic-inorganic synthesis of mixed oxides. J.Am.Ceram.Soc. 1999; 82: 556-560.
[14] Gardiner R, Brown D W and Kirlin P S, Volatile barium beta-diketonate polyether adducts - synthesis, characterization, and metalloorganic chemical vapor-deposition. Chem.Mater. 1991; 3: 1053-1059.
[15] Han S, Kim C and Kwon D, Thermal/oxidative degradation and stabilization of polyethylene glycol. Polymer 1997; 38: 317-323.
[16] Roura P, Farjas J, Eloussifi H, Carreras L, Ricart S, Puig T and Obradors X, Thermal analysis of metal organic precursors for functional oxide preparation: Thin films versus powders. Thermochim.Acta 2015; 601: 1-8.
[17] Aguirre J M, Gutierrez A and Giraldo O, J.Braz.Chem.Soc. 2011; 22: 546-551.

[18] Melnikov P, Nascimento V A, Consolo L Z Z and Silva A F, Mechanism of thermal decomposition of yttrium nitrate hexahydrate, Y(NO3)(3)center dot 6H(2)O and modeling of intermediate oxynitrates. J.Term.Anal.Calorim. 2013; 111: 115-119.

[19] Chu P -Y and Buchanan R C, Reactive liquid-phase sintering of YBa2Cu3O7-x superconducting thin-films .2. Sintering mechanism and film properties. J.Mater.Res. 1994; 9: 844-851.

[20] Vermeir P, Feys J, Schaubroeck J, Verbeken K, Lommens P and Van Driessche I, Influence of sintering conditions in the preparation of acetate-based fluorine-free CSD YBCO films using a direct sintering method. Mater.Res.Bull. 2012; 47: 4376-4382.

[21] Vermeir P, Cardinael I, Schaubroeck J, Verbeken K, Bäcker M and Lommens P, Elucidation of the Mechanism in Fluorine-Free Prepared YBa2Cu3O7-delta Coatings. Inorg.Chem. 2010; 49: 4471-4477.

[22] Nevriva M, Pollert E, Matejkova L and Triska A, On the determination of the CuO-BaCuO2 and CuO-YCuO2.5 binary phase-diagrams. J.Cryst.Growth 1988; 91: 434-438.

[23] Soler L et al. submitted.

[24] Zhang W, Osamura K and Ochiai S, Phase-diagram of the BaO-CuO binary-system. J.Am.Ceram.Soc. 1990; 73: 1958-1964.

[25] Lander J J, Polymorphism and anion rotational disorder in the alkaline earth carbonates. J.Chem.Phys. 1949; 17: 892-901.

[26] Judd M D and Pope M I, Transition temperatures for (Sr, Ba)CO3: a possible DTA temperature standard. Thermochim.Acta 1973; 7: 247-248.

[27] Chu J, Zhao Y, Ji Y, Wu W, Shi J, Hong Z, Ma L, Suo H and Jin Z, Interface reaction-governed heteroepitaxial growth of YBa2Cu3O7-δ film on CeO2-buffered technical substrate. J.Am.Ceram.Soc. 2019; 102: 5705–5715.

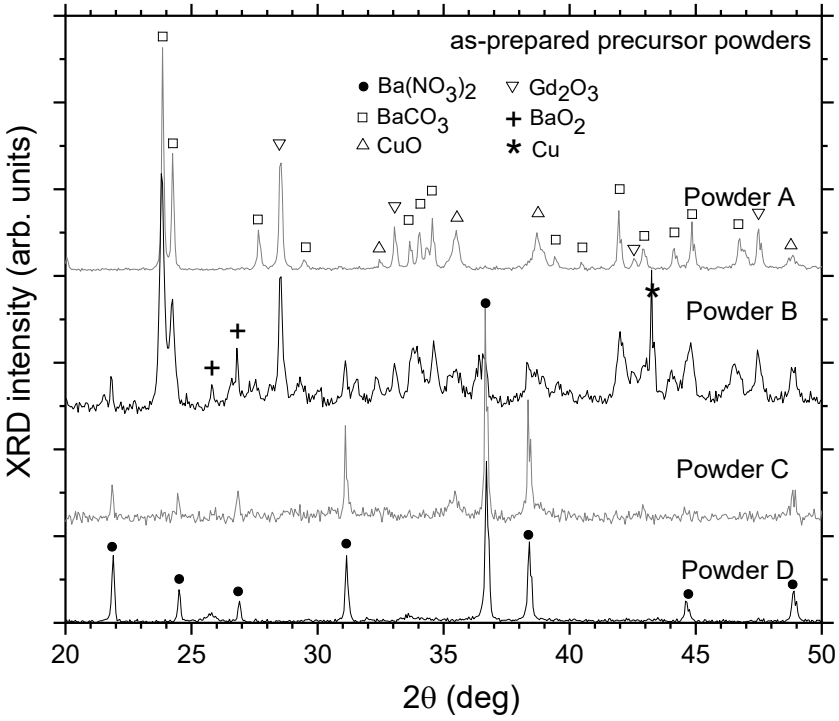

Figure 1.- XRD curves of the as-prepared precursor powders.

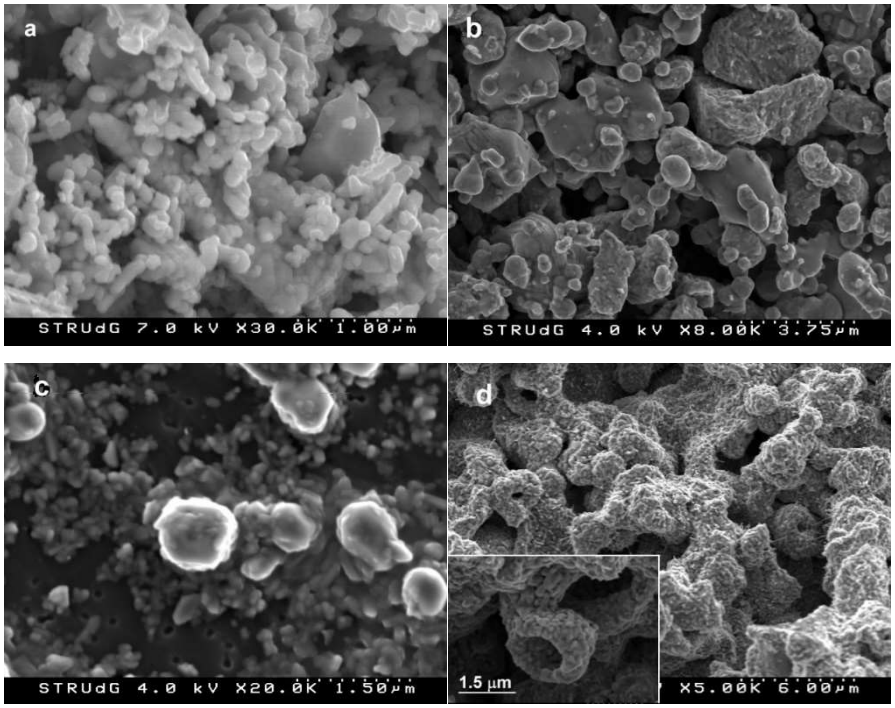

Figure 2.- SEM microphotographs of the ceramic Powder A after grinding (a) and after 5 min at 900ºC (b). Idem for the the spray-dried Power D after drying (c) and after 5 min at 900ºC (d).

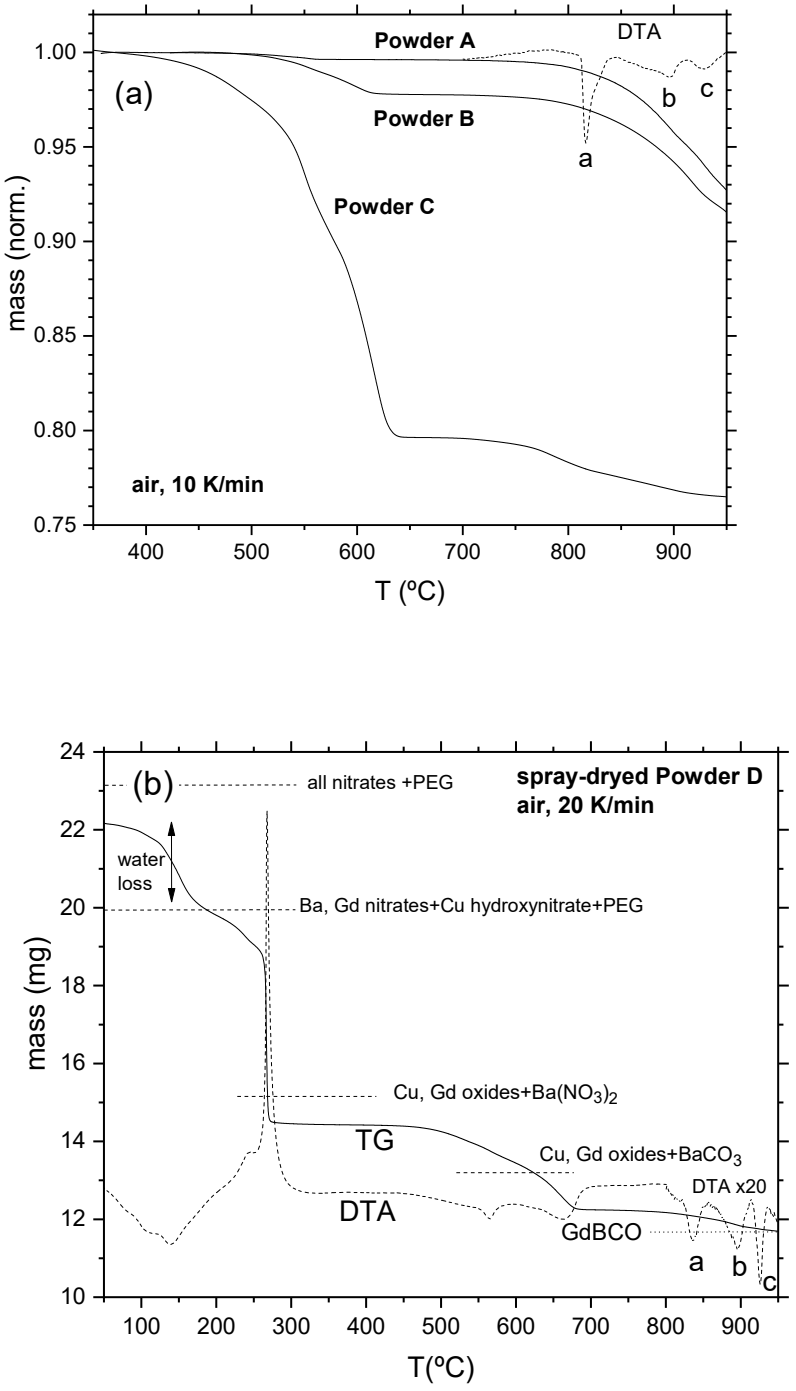

Figure 3.- a) TG curves measured on Powders A, B and C. The mass is normalized at the value at 450ºC. DTA curve of Powder A is also plotted. When heated again, peak "a" was still detected but much less intense. b) TG/DTA curves (solid/dashed) measured on Powder D. The value of the absolute mass is represented. Above 800ºC the DTA signal has been expanded (x20) to show the small endothermic peaks leading to formation of GdBCO. When heated again, all these peaks disappeared.

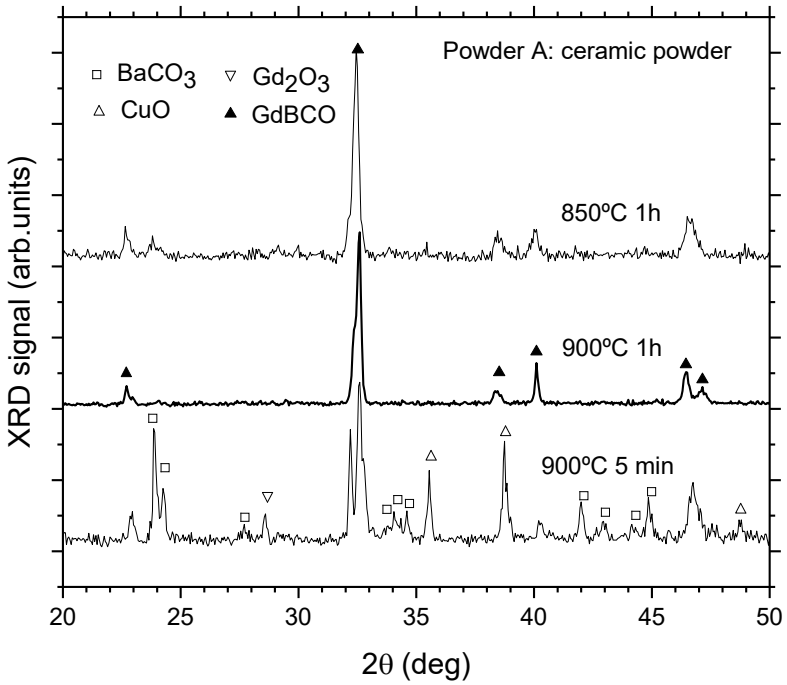

Figure 4.- XRD of Powder A after heat-treating at 850 and 900ºC for 1 h.

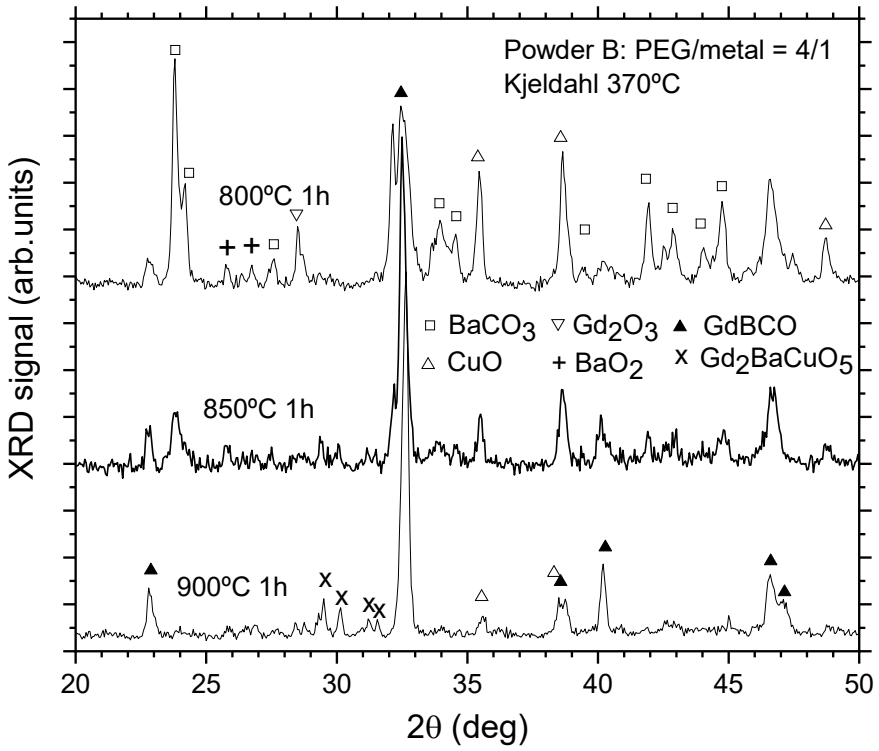

Figure 5.- XRD of Powder B after heat-treating at several temperatures.

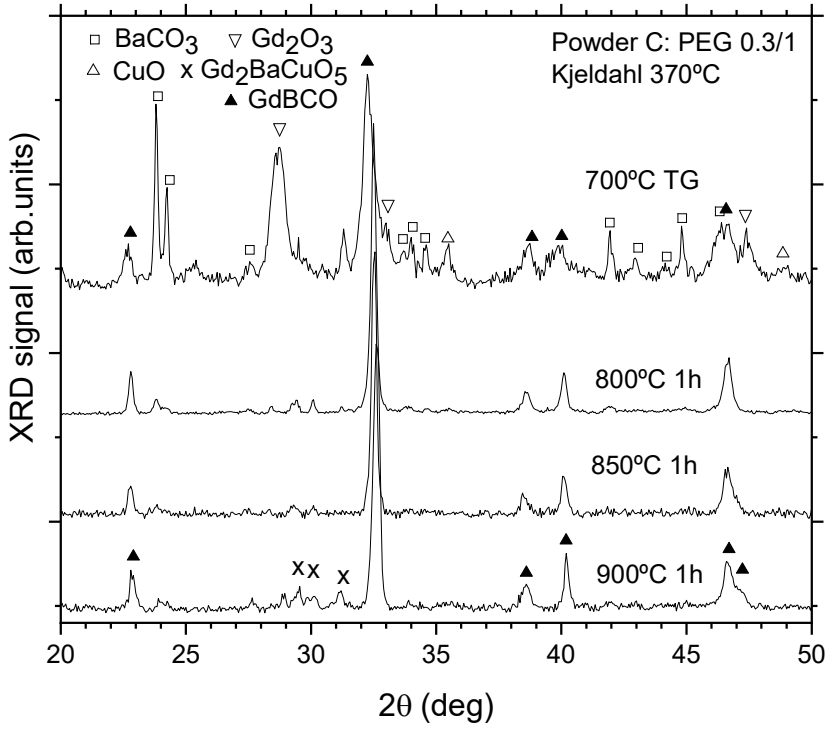

Figure 6.- XRD of Powder C after heat-treating at several temperatures. The curve labelled "700ºC TG" was measured after heating at 10 K/min without any isothermal stage.

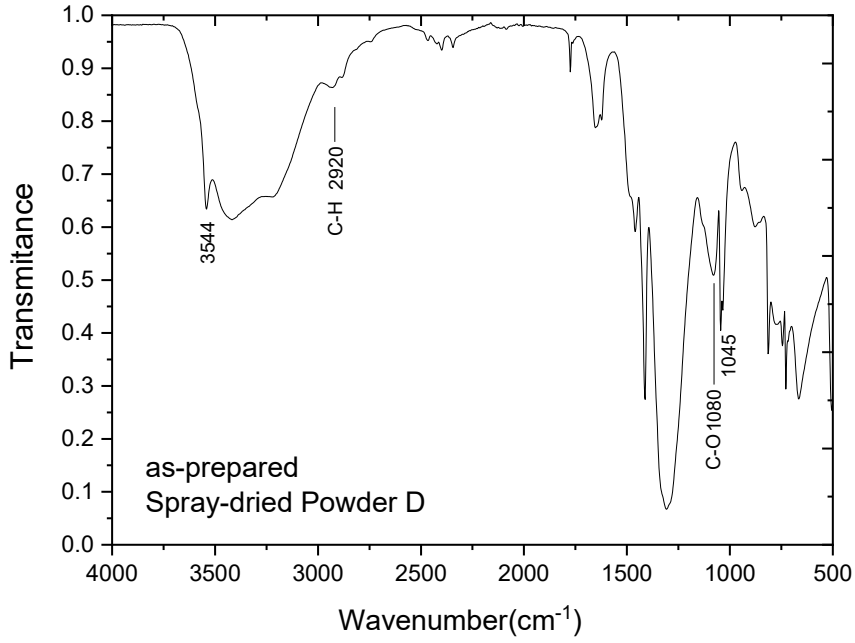

Figure 7.- FTIR spectrum of the spray-dried precursor Powder D.

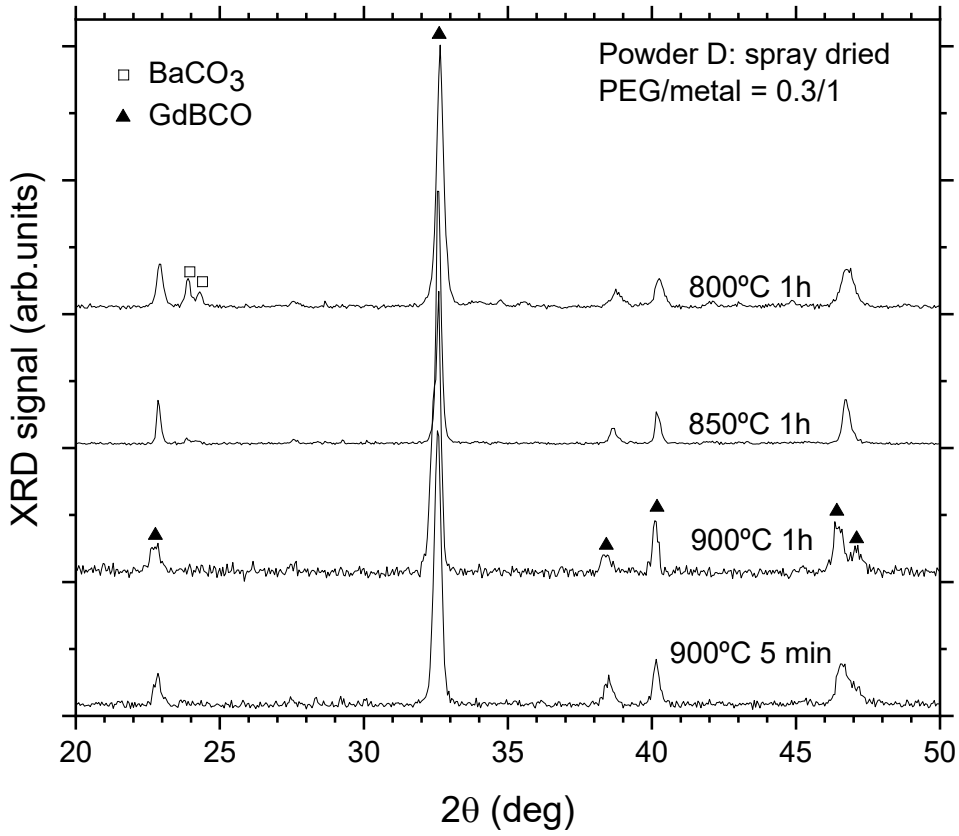

Figure 8.- XRD of Powder D after heat-treating at several temperatures.

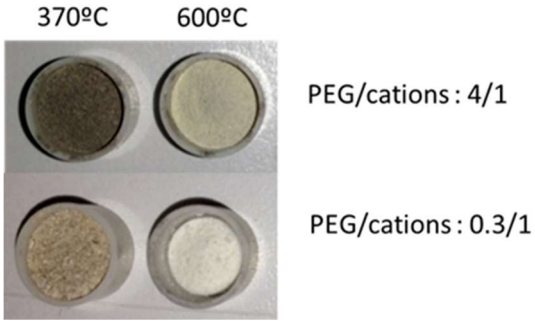

Figure 9.- Optical aspect of the "binary" (without copper) precursor powders B (4/1) and C (0.3/1) as precipitated (left) and after heating them at 600ºC for 1 h in air (right). The brighter aspect of the powder with less PEG indicates that less carbonaceous residue is produced.